Statistical model analysis of α-induced reaction cross sections of ^{64}Zn at low energies

P. Mohr,[1,2,*] Gy. Gyürky,[1] and Zs. Fülöp[1]
[1]*Institute for Nuclear Research (MTA Atomki), H-4001 Debrecen, Hungary*
[2]*Diakonie-Klinikum, D-74523 Schwäbisch Hall, Germany*
(Received 16 December 2016; published 26 January 2017)

Background: α-nucleus potentials play an essential role in the calculation of α-induced reaction cross sections at low energies in the statistical model. Uncertainties of these calculations are related to ambiguities in the adjustment of the potential parameters to experimental elastic scattering angular distributions (typically at higher energies) and to the energy dependence of the effective α-nucleus potentials.
Purpose: The present work studies cross sections of α-induced reactions for ^{64}Zn at low energies and their dependence on the chosen input parameters of the statistical model calculations. The new experimental data from the recent Atomki experiments allow for a χ^2-based estimate of the uncertainties of calculated cross sections at very low energies.
Method: Recently measured data for the (α,γ), (α,n), and (α,p) reactions on ^{64}Zn are compared to calculations in the statistical model. A survey of the parameter space of the widely used computer code TALYS is given, and the properties of the obtained χ^2 landscape are discussed.
Results: The best fit to the experimental data at low energies shows $\chi^2/F \approx 7.7$ per data point, which corresponds to an average deviation of about 30% between the best fit and the experimental data. Several combinations of the various ingredients of the statistical model are able to reach a reasonably small χ^2/F, not exceeding the best-fit result by more than a factor of 2.
Conclusions: The present experimental data for ^{64}Zn in combination with the statistical model calculations allow us to constrain the astrophysical reaction rate within about a factor of 2. However, the significant excess of χ^2/F of the best fit from unity demands further improvement of the statistical model calculations and, in particular, the α-nucleus potential.

DOI: 10.1103/PhysRevC.95.015807

I. INTRODUCTION

Statistical model (StM) calculations are widely used for the calculation of reaction cross sections of α-induced reactions for intermediate-mass and heavy target nuclei. It is found that the cross sections at low energies depend sensitively on the chosen α-nucleus optical model potential. These low-energy cross sections play also an essential role under stellar conditions. In particular, (γ,α) photodisintegration reactions in the so-called astrophysical p process (or γ process) are best determined by study of the inverse (α,γ) capture reactions [1]. Under typical p-process conditions, temperatures of about 2 billion to 3 billion kelvins are reached (in short, $T_9 = 2$–3), and the corresponding Gamow window is located at a few MeV for intermediate-mass nuclei like ^{64}Zn (e.g., [2–6]).

The lightest nucleus which is synthesized in the p process is ^{74}Se [2]. These so-called p nuclei are typically characterized by very low natural abundances, of the order of 1% or even below. Although ^{64}Zn is somewhat lighter than the lightest p nucleus, it has nevertheless been chosen for the present study because the cross sections of various α-induced reactions can be determined for ^{64}Zn by the simple and robust activation technique with a high precision. The high natural abundance of ^{64}Zn, almost 50%, allows us to use targets with a natural isotopic composition. However, there is also a drawback. For lighter nuclei like ^{64}Zn the applicability of the StM may be limited at very low energies because of an insufficient level density in the ^{68}Ge compound nucleus.

Our recent study of α-induced reaction cross sections for the target nucleus ^{64}Zn [7,8] focused on total reaction cross sections $\sigma_{\rm reac}$ and their determination either from the elastic scattering angular distributions or from the sum over the cross sections of all open nonelastic channels (including inelastic scattering). It was found that there is excellent agreement at the lower energy of 12.1 MeV (428 ± 7 mb from elastic scattering vs 447 ± 41 mb from the sum over nonelastic channels). At the higher energy of 16.1 MeV a significant contribution of compound-inelastic (α,α') scattering to higher-lying states in ^{64}Zn was identified, which is about 15%–20% of the $\sigma_{\rm reac} = 905 \pm 18$ mb from elastic scattering.

The present study extends our previous work [7,8] by a detailed study of the (α,γ), $(\alpha,{\rm n})$, $(\alpha,{\rm p})$, and total reaction cross sections and their dependence on the underlying parameters of the StM calculations. For this purpose the full parameter space of the widely used TALYS [9] code (version 1.8) is investigated. In particular, all available options for the α-nucleus optical model potential (A-OMP), the nucleon OMP (N-OMP), the γ-ray strength function (GSF), and the level density (LD) are varied. Almost 7000 combinations of input parameters are used to calculate a χ^2 landscape. This landscape provides improved insight into the sensitivities of the different reaction channels to the underlying parameters. It is the scope of the present study to obtain an improved χ^2-based prediction of reaction cross sections at very low energies where experimental data are not available. As an example,

*mohr@atomki.mta.hu

an extrapolation to the astrophysically most relevant energies is made for the ^{64}Zn$(\alpha,\gamma)^{68}$Ge reaction, with an estimate of the corresponding uncertainties.

The most important ingredient for the calculation of α-induced reaction cross sections in the StM is the A-OMP. For heavy nuclei (above $A \gtrsim 100$) it has been found that different A-OMPs lead to dramatic variations of the predicted cross sections, exceeding one order of magnitude at astrophysically relevant energies (e.g., [10,11]). On the contrary, a quite reasonable description of the recent data for ^{64}Zn was found for several A-OMPs [7]. However, as shown below from a χ^2-based assessment, this reasonable description for ^{64}Zn is still far from a precise prediction of the experimental results.

The paper is organized as follows. In Sec. II a brief description of the statistical model and its ingredients is given. Available experimental data are summarized in Sec. III. Section IV presents the results and shows the obtained excitation functions for the total reaction cross section $\sigma_{\rm reac}$ and the (α,γ), $(\alpha,{\rm n})$, and $(\alpha,{\rm p})$ reaction channels under study. A discussion of the results and an extrapolation to lower energies are provided in Sec. V. Conclusions are drawn in Sec. VI.

II. PARAMETERS OF THE STATISTICAL MODEL

A. Basic considerations

In schematic notation the reaction cross section in the StM is proportional to

$$\sigma(\alpha,X) \sim \frac{T_{\alpha,0}T_X}{\sum_i T_i} = T_{\alpha,0} \times b_X, \tag{1}$$

with the transmission coefficients T_i into the ith open channel and the branching ratio $b_X = T_X/\sum_i T_i$ for the decay into channel X. The total transmission is given by the sum over all contributing channels: $T_{\rm tot} = \sum_i T_i$. The T_i's are calculated from global optical potentials (A-OMP and N-OMP for the particle channels) and from the GSF for the photon channel. The T_i's include the contributions of all final states j in the respective residual nucleus in the ith exit channel. In practice, the sum over all final states j is approximated by the sum over low-lying excited states up to a certain excitation energy $E_{\rm LD}$ (these levels are typically known from experiment) plus an integration over a theoretical level density for the contribution of higher-lying excited states:

$$T_i = \sum_j T_{i,j} \approx \sum_j^{E_j<E_{\rm LD}} T_{i,j} + \int_{E_{\rm LD}}^{E_{\rm max}} \rho(E)\,T_i(E)\,dE. \tag{2}$$

For further details of the definition of T_i, see [12]. $T_{\alpha,0}$ refers to the entrance channel, where the target nucleus is in its ground state under laboratory conditions. Calculation of the stellar reaction rates $N_A\langle\sigma v\rangle$ requires further modifications of Eq. (1) which have to take into account thermal excitations of the target nucleus [12]. For the (α,γ) reaction of the even-even nucleus ^{64}Zn with the relatively high excitation energy of the first excited state ($J^\pi = 2^+$, $E^* = 992$ keV), these corrections remain small at typical temperatures of the p process of the order of a few billion kelvins [13,14].

The properties of the T_i in Eqs. (1) and (2) lead to the following general findings for the case of ^{64}Zn. At very low energies, the (α,γ) channel with its positive Q value of $Q_\gamma = +3.40$ MeV is the only open reaction channel besides elastic and inelastic scattering. The transmission T_γ into the γ channel exceeds the transmission T_α into the α channel, which is strongly suppressed by the Coulomb barrier. Consequently, $\sum_i T_i \approx T_\gamma$, and the (α,γ) cross section becomes proportional to $T_{\alpha,0}$ but almost independent of the other T_i's (including T_γ).

As soon as the proton channel opens ($Q_p = -3.99$ MeV), T_p increases almost exponentially with the energy and exceeds T_γ already close above the proton threshold. Because of the lower Coulomb barrier for the proton channel (compared to the α case), T_p becomes the dominant contributor to the sum in $T_{\rm tot}$. This leads to an $(\alpha,{\rm p})$ cross section proportional to $T_{\alpha,0}$ but independent of the other T_i's (including T_p). The (α,γ) cross section becomes approximately proportional to $T_{\alpha,0}T_\gamma/T_p$.

Because of the strongly negative Q value of the $(\alpha,{\rm n})$ channel ($Q_n = -8.99$ MeV) and the resulting smaller phase space [in comparison to the $(\alpha,{\rm p})$ reaction], the contribution of the $(\alpha,{\rm n})$ channel remains relatively small. This finding is different from that in heavy nuclei, where the $(\alpha,{\rm n})$ channel typically becomes dominant close above the neutron threshold (see, e.g., [15]). Now we find the approximate proportionalities of $T_{\alpha,0}T_p/(T_p+T_n)$ for the $(\alpha,{\rm p})$ cross section, $T_{\alpha,0}T_n/(T_p+T_n)$ for the $(\alpha,{\rm n})$ cross section, and $T_{\alpha,0}T_\gamma/(T_p+T_n)$ for the (α,γ) cross section.

Although the above discussion is indeed somewhat simplistic, it is nevertheless helpful for a general understanding of the sensitivities of the (α,γ), $(\alpha,{\rm n})$, and $(\alpha,{\rm p})$ cross sections to the underlying parameters. Sensitivities as a function of energy have been calculated by Rauscher [16] for a wide range of nuclei; the results from the NON-SMOKER code are available online at [17] and confirm the above discussion for ^{64}Zn.

The role of the level density requires further discussion. As Eq. (2) shows, the chosen parametrization of the LD becomes relevant only above a certain number of low-lying excited states, which are taken into account explicitly. Typically, these low-lying levels cover an excitation energy range of $E^* \approx$ 2–3 MeV. Thus, for α-induced reactions on ^{64}Zn this means that the importance of the LDs remains limited, in particular, at low energies, for the $(\alpha,{\rm n})$ and $(\alpha,{\rm p})$ reactions, whereas the role of the LD is significant for the (α,γ) reaction; here the last term in Eq. (2) does contribute.

However, besides its relatively minor role in the calculation of the transmissions T_i in Eq. (2), the LD plays an essential role in the applicability of the StM, which is valid only if the experimental conditions (mainly the target thickness and energy distribution of the beam) average over a sufficient number of levels in the compound nucleus ^{68}Ge. For the present data the energy interval ΔE of the experiment is of the order of 100 keV [8]. The experimental energies cover an energy range of about 6 MeV $\leqslant E_{\rm c.m.} \leqslant$ 15 MeV. Together with the Q value of the (α,γ) reaction, about +4 MeV, this corresponds to excitation energies E^* in ^{68}Ge of about 10 MeV $\leqslant E^* \leqslant$ 19 MeV.

The various options for the LD in TALYS (see Sec. II B 4) predict total level densities (per parity) of between about 9000 and 80 000 MeV^{-1} already at the lowest energies under study. At first glance, this seems to be sufficient for the applicability of the StM. But particularly for the $(\alpha,{\rm p})$ reaction

slightly above the threshold, the experimental excitation curve is not completely smooth (as expected for fully statistical behavior). Slightly above the threshold, the ^{64}Zn(α,p)^{67}Ga reaction populates only very few final states in ^{67}Ga, with low spins J and negative parity. The barrier penetration in this exit channel favors proton emission with a low angular momentum, and thus by far not all levels in the ^{68}Ge compound nucleus contribute to the ^{64}Zn(α,p)^{67}Ga cross section. A closer look at the LDs in ^{68}Ge shows that the predicted LD per spin goes down to, e.g., about a few hundred per MeV for $J = 0$, or less than 100 levels may contribute to the averaging within the experimental energy interval of $\Delta E \approx 100$ keV. Thus, nonstatistical fluctuations in the excitation function of ^{64}Zn(α,p)^{67}Ga at low energies are not very surprising.

LDs increase dramatically with increasing excitation energy. At the highest energies under study, the predicted LDs are at least two orders of magnitude higher than at the lowest energies. And indeed the nonstatistical fluctuations in the excitation function of ^{64}Zn(α,p)^{67}Ga disappear at energies above 10 MeV (corresponding to $E^* \approx 14$ MeV in ^{68}Ge, or an increase in the level density by more than one order of magnitude, compared to $E^* \approx 10$ MeV).

B. Ingredients under consideration

1. α-nucleus optical model potentials

The α-nucleus optical model potential is the essential ingredient for the calculation of α-induced reaction cross sections at low energies. TALYS provides eight options for the A-OMP: The first option is based on the early work of Watanabe [26]; this was the default option in TALYS. The widely used simple four-parameter potential of McFadden and Satchler [27] is the second option in TALYS. Three versions of the double-folding A-OMP of Demetriou *et al.* [28] (DGG-1, DGG-2, DGG-3) are also included in TALYS. Since TALYS version 1.8, three additional A-OMPs are available, which are based on Nolte *el al.* [29] and on two versions by Avrigeanu *et al.* [30,31] (AVR for the latest version in [30]).

In addition, the new ATOMKI-V1 potential [32] was implemented in the TALYS code, and modifications of the third version of the Demetriou potential DGG-3 were investigated. It was recently suggested in [10] that the real part of this potential should be multiplied by a factor of about $N_{\rm DGG} \approx 1.1$–1.2 for a better description of reaction data for heavy targets ($A \gtrsim 100$). For ^{64}Zn is shown that the best fit is achieved by a reduction of the real part by a factor of about 0.9 (instead of an increased potential as found for $A \gtrsim 100$ in [10]).

The latest global A-OMP, by Su and Han [33], is not yet implemented in TALYS. It is shown in [7] that this potential overestimates the total reaction cross sections for ^{64}Zn at low energies. Thus, no efforts have been made to implement this potential in TALYS for the present study.

2. Nucleon-nucleus optical model potentials

The default option in TALYS is based on the local and global parametrizations of Koning and Delaroche [34]. Furthermore, based on the work of Jeukenne, Lejeune, and Mahaux (e.g., [35]), four versions of the so-called JLM potential are available. The basic JLM-type potential is taken from Bauge *et al.* [36], and three modifications of this potential are taken from Goriely and Delaroche [37].

3. γ-ray strength functions

Eight options for the γ-ray strength function are implemented in TALYS. In general, the options are based on the work of Brink [38] and Axel [39] or Kopecky and Uhl [40]. In addition, microscopic model GSFs have been calculated on the basis of the Hartree-Fock BCS, Hartree-Fock-Bogolyubov, and relativistic mean-field models [41] and a hybrid model [42]. Furthermore, the above choices can be combined with two options for the M1 strength function when the M1 strength is either normalized to the E1 strength (default option) or not normalized. A detailed description of the available options can be found in the TALYS manual [9] and in the Reference Input Parameter Library (RIPL) [41].

4. Level densities

Three phenomenological and three miscroscopic level densities can be chosen in TALYS. The phenomenological options are based on constant-temperature and back-shifted Fermi gas models and on the generalized superfluid model. The microscopic approaches are calculated using Skyrme- or Gogny-type forces. Details on the various options are summarized in [43].

III. EXPERIMENTAL DATA

Several excitation functions of α-induced reaction cross sections for ^{64}Zn are available in the literature and in the EXFOR database [18]. However, either the data are more than 50 years old [19–22] or the data have not been published in refereed journals [23–25]. All EXFOR data are presented in Fig. 1. Unfortunately, significant discrepancies between the different excitation functions are found (see Fig. 1).

Although there is no good agreement between the different experimental data sets, Fig. 1 nicely shows that the overall energy dependence of the various reaction channels is well reproduced by the best-fit statistical model calculation. The only exceptions are the (α,3n) reaction, where the only available experimental data set, that of Porile [19], is more than one order of magnitude higher than the theoretical estimate, and the (α,2n) reaction, which is underestimated by about a factor of 4.

Furthermore, the importance of the various reaction channels at different energies can be read nicely from Fig. 1. At very low energies, below about 6 MeV the (α,γ) reaction dominates because the (α,p) and (α,n) channels are closed or suppressed by the Coulomb barrier of the outgoing low-energy proton. At about 6 MeV the (α,p) reaction starts to dominate, up to almost 20 MeV. As soon as the (α,n) channel opens, also a significant contribution of the (α,n) channel is found. Above 20 MeV, various multiparticle emission channels like (α,pn), (α,2n), and (α,αn) contribute also to the total reaction cross section $\sigma_{\rm reac}$.

As the focus of the present study is the low-energy region, we finally decided to use only our latest data on the

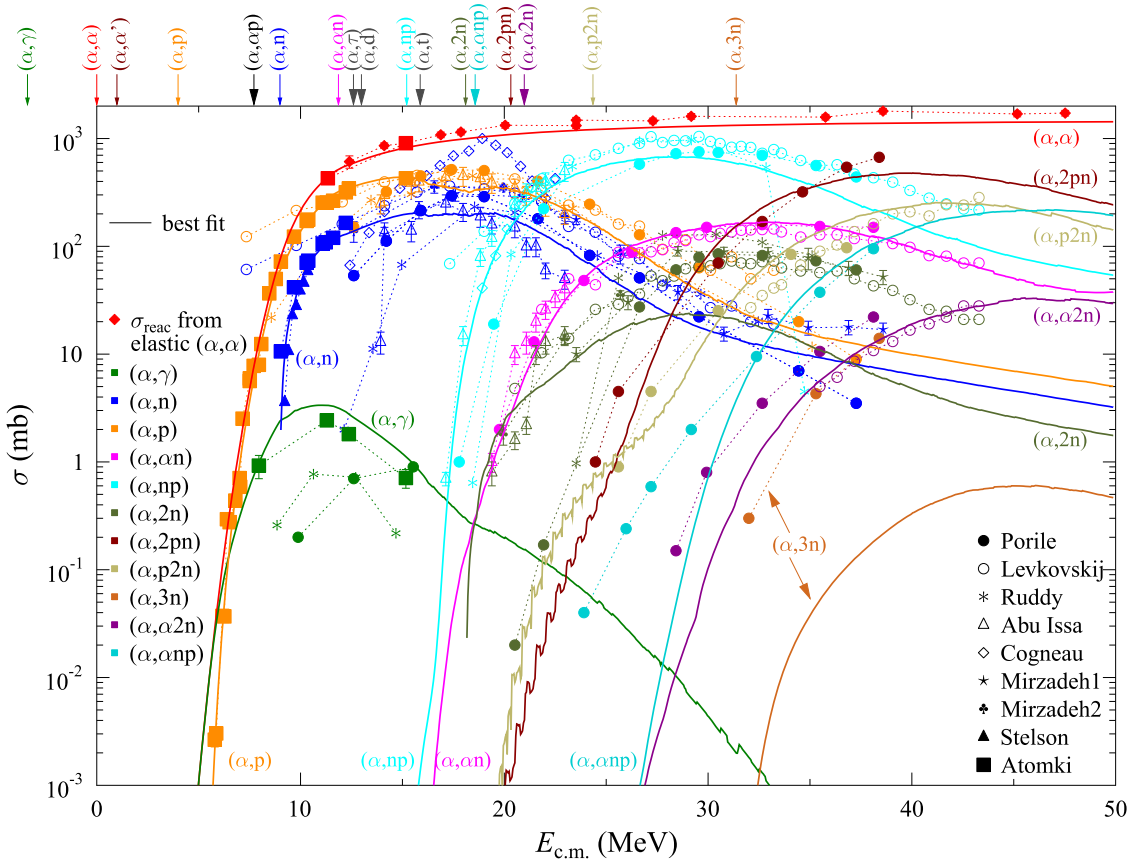

FIG. 1. Cross sections of α-induced reactions on ^{64}Zn over a wide energy range. Data labeled σ_{reac} (in red) are total reaction cross sections and are derived from elastic scattering angular distributions [7]. Thresholds for the different channels are indicated by the arrows at the top. Data sets for different reaction channels are shown in different colors: (α,γ) reaction, in green; $(\alpha$,n), in blue; and $(\alpha$,p), in orange. Different symbols represent the data sets of Porile [19], Levkovskij [25], Ruddy *et al.* [20], Abu Issa *et al.* [23], and Cogneau *et al.* [22], Mirzadeh *et al.* (two data sets) [24], and Stelson *et al.* [21] and the recent Atomki data [7,8]. All data sets are connected by thin dotted lines to guide the eye. Solid lines are the best-fit TALYS calculations (see Sec. IV). For further discussion see the text.

α-induced cross sections for ^{64}Zn for determination of the best-fit parameters for the statistical model calculations at low energies. In particular, this means 4 data points for the (α,γ) reaction, 10 data points for the $(\alpha$,n) reaction, 27 data points for the $(\alpha$,p) reaction, and 2 data points for the total reaction cross section σ_{reac} from the analysis of the elastic scattering angular distributions [7,8]; in total, 43 experimental data points are used to determine the χ^2 landscape. The χ^2 adjustment procedure is discussed in detail in the following section.

IV. RESULTS FOR χ^2/F

All combinations of the A-OMPs, N-OMPs, GSFs, and LD parametrizations in Sec. II B have been used for calculation of the (α,γ), $(\alpha$,n), and $(\alpha$,p) cross sections of ^{64}Zn. In detail this means that 6720 combinations of A-OMPs, N-OMPs, GSFs, and LDs have been calculated. This number results from 14 A-OMPs (8 built-in in TALYS plus ATOMKI-V1 plus DGG-3 multiplied by factors of $N_{\text{DGG}} = 0.7$, 0.8, 0.9, 1.1, and 1.2), 8 E1 GSFs combined with two additional options for the M1 strength, 5 N-OMPs, and 6 LDs.

Technically it would be possible to increase this number further by choosing different models for each residual nucleus, e.g., different N-OMPs for the neutron and the proton channel and different GSFs or LDs for even and odd residual nuclei. However, best-fit parameters should be valid for a reasonable range of nuclei, and thus the present work intentionally remains restricted to the above-listed 6720 combinations of A-OMPs, N-OMPs, GSFs, and LDs and does not apply different parameter sets for different residual nuclei of the $\alpha + ^{64}$Zn reactions.

For each of the 6720 combinations of parameters, excitation functions for the total reaction cross section σ_{reac} and the cross sections of the (α,γ), $(\alpha$,n), and $(\alpha$,p) reaction channels were calculated, and the deviation between the theoretical excitation functions and the experimental data was determined by a standard χ^2 calculation.

A. χ^2/F from all experimental data points

It is found that the 6720 combinations under study show a wide range of χ^2/F per data point, from slightly below 8 to more than 4000 for all 43 experimental values for σ_{reac} and the $(\alpha$,n), (α,γ), and $(\alpha$,p) reactions in [7] and [8]. These χ^2/F values correspond to an average deviation factor f_{dev} between experiment and theory for all data points, from about 1.3 for

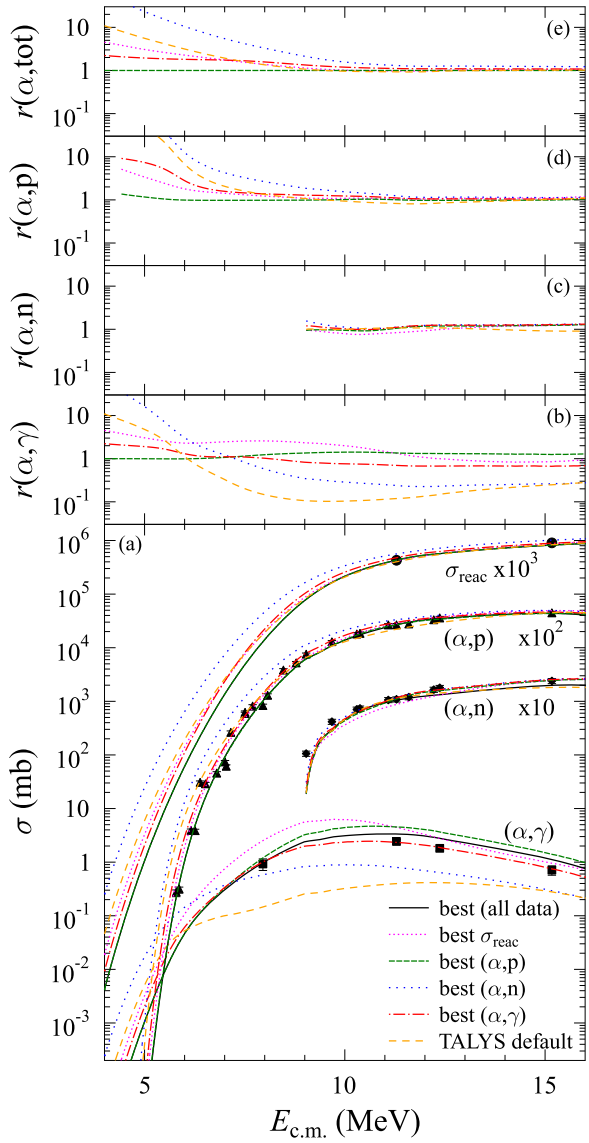

FIG. 2. Cross sections of α-induced reactions on ^{64}Zn; for better readability, the total reaction cross sections $\sigma_{\rm reac}$ have been multiplied by a factor of 1000, the (α,p) data by a factor of 100, and the (α,n) data by a factor of 10. The best fit of all 6720 combinations of the TALYS parameters is shown by the solid black line. Best fits to the $\sigma_{\rm reac}$ data are represented by the narrow-dotted magenta line; to the individual (α,p) reaction, by the dashed green line; to the individual (α,n) reaction, by the dotted blue line; and to the individual (α,γ) reaction, by the dash-dotted red line. The TALYS default calculation is shown by the short-dashed orange line. (a) Calculated excitation functions in comparison to the experimental data. For better visualization, (b)–(e) show the same calculations as a ratio r for a particular (α,X) channel, normalized to the overall best-fit calculation. For example, (b) shows the (α,γ) cross sections from the best fits to the (α,γ), (α,n), (α,p), and $\sigma_{\rm reac}$ data, normalized to the overall best fit. For further discussion see the text.

the best fits up to 2.6 for the worst cases. Figure 2 shows the results of the above calculations. The smallest $\chi^2/F \approx 7.7$ per point was found for the following combination: the A-OMP was derived from the DGG-3 potential with the real part multiplied by a factor of $N_{\rm DGG} = 0.9$; the N-OMP is taken from Koning and Delaroche (TALYS default); the GSF is calculated using the Brink-Axel Lorentzian model with unnormalized M1 strength; and the LD was taken from the back-shifted Fermi gas model. The obtained $\chi^2/F \approx 7.7$ corresponds to $f_{\rm dev} \approx 1.3$. Obviously, a $\chi^2/F \approx 7.7$ corresponds on average to almost a 3σ deviation for each data point, which is not fully satisfying. This finding is discussed later (see Sec. V). Furthermore, it must be pointed out that this best fit is indeed restricted to the low-energy data. At higher energies, above about 15 MeV the DGG-3 A-OMP underestimates the total reaction cross sections $\sigma_{\rm reac}$ significantly, and this deviation increases with decreasing normalization factor $N_{\rm DGG}$ ($N_{\rm DGG} = 0.9$ for the best fit); see also Fig. 1.

The four experimental data points for the (α,γ) reaction are reproduced with χ^2/F from 0.1 up to more than 1200, corresponding to $f_{\rm dev} \approx 1.05$–8. The χ^2/F for the 10 (α,n) data points show a much smaller variation of χ^2/F, from 4.7 to 16.3, corresponding to $f_{\rm dev}$ between 1.2 and 1.9. The 27 data points for the (α,p) reaction show a wide variation of χ^2/F, from 6.6 to 6500, corresponding to $f_{\rm dev}$ between 1.25 and 3.2. Finally, because of the small experimental uncertainties, the total reaction cross sections $\sigma_{\rm reac}$ show a significant χ^2/F between 2.9 and 200 although $f_{\rm dev}$ remains relatively close to unity between 1.03 and 1.21. For completeness it must be mentioned that the total reaction cross section $\sigma_{\rm reac}$ is sensitive only to the A-OMP, and independent of the other ingredients of the StM calculations.

B. χ^2/F from the individual reaction channels

In addition, Fig. 2 shows the best fits to the particular (α,p), (α,n), and (α,γ) channels. Obviously, as soon as the fit is restricted to a particular (α,X) reaction, the resulting parameters are different. This becomes, e.g., very prominent for the (α,γ) reaction, which depends sensitively on the combination of the transmission coefficients of different α, n, p, and γ channels.

The cross sections in Fig. 2 show a strong energy dependence, and they cover several orders of magnitude. Thus, for better visualization we have also included the ratios r between the individual fits and the best fit for each of the (α,γ), (α,n), and (α,p) channels in Figs. 2(b)– 2(e). Figure 2(c) nicely shows the minor sensitivity of the (α,n) cross section. In Fig. 2(d) it is obvious that the dominating (α,p) cross section shows a strong sensitivity to the chosen parameters at low energies, whereas Fig. 2(b) shows that the (α,γ) cross section varies widely over the whole energy range under study. Consequently, improved constraints for the StM parameters could be obtained from (α,p) data towards lower energies (down to threshold) and from (α,γ) data with smaller uncertainties over the full energy range.

1. χ^2/F from (α,γ) data

The lowest $\chi^2/F \approx 0.13$ for the (α,γ) channel is obtained for the combination of A-OMP: DGG-3 with $N_{\rm DGG} = 1.2$; N-OMP: Koning and Delaroche (TALYS default); GSF: hybrid model, M1 strength not normalized; and LD: constant-temperature Fermi gas (TALYS default). However, the

best-fit parameters of the (α,γ) channel lead to an increased χ^2/F for all $\sigma_{\rm reac}$, $(\alpha,{\rm p})$, $(\alpha,{\rm n})$, and (α,γ) data by more than a factor of 5 to about 40 (compared to 7.7 for the overall best fit), and in particular, the $(\alpha,{\rm p})$ cross section at low energies is about a factor of 10 higher than the overall best fit [see Fig. 2(d)]. Here it becomes evident that a restricted analysis of the (α,γ) channel only may be misleading. The (α,γ) cross section is sensitive to the combination of several ingredients of the StM calculation, and a shortcoming of a particular ingredient of the StM may, at least partly, be compensated by a further shortcoming of another ingredient.

2. χ^2/F from (α,n) data

The cross section of the $(\alpha,{\rm n})$ reaction is governed by its significantly negative Q value, about -9 MeV, and the resulting phase space at energies close above the threshold. The sensitivity to all parameters remains limited, and for all 6720 combinations χ^2/F remains within 4.7 and 16.3. The low sensitivity of the $(\alpha,{\rm n})$ cross section can also be seen in Fig. 2(c). The lowest $\chi^2/F \approx 4.7$ is found for A-OMP: Nolte potential [29]; N-OMP: Koning and Delaroche (TALYS default); GSF: Kopecky-Uhl generalized Lorentzian, with normalized M1 strength; and LD: microscopic, from Skyrme force, Hilaire's combinatorial tables. For the $(\alpha,{\rm n})$ fit the overall χ^2/F increases significantly, by more than two orders of magnitude, to 1265; i.e., because of the reduced sensitivity of the $(\alpha,{\rm n})$ cross section, it is practically impossible to constrain the parameters of the StM calculations from the $(\alpha,{\rm n})$ data.

3. χ^2/F from (α,p) data

The $(\alpha,{\rm p})$ reaction dominates in the energy range under study, and by far the most data points are available for this channel. It is not surprising that the fit of the $(\alpha,{\rm p})$ data leads to a combination of parameters which is close to the overall best fit. Here we find A-OMP: DGG-3 with $N_{\rm DGG} = 0.9$; N-OMP: Koning and Delaroche (TALYS default); GSF: Brink-Axel Lorentzian, M1 normalized; and LD: microscopic, from Skyrme force, Hilaire's combinatorial tables. A $\chi^2/F \approx 6.6$ is achieved for the $(\alpha,{\rm p})$ channel, and the overall χ^2/F increases only slightly, to about 11.4 (compared to 7.7 for the best fit). However, the $(\alpha,{\rm p})$ fit leads to a significant overestimation of the (α,γ) channel, leading to a $\chi^2/F \approx 54$ for the few data points for the (α,γ) channel.

4. χ^2/F from $\sigma_{\rm reac}$ data

The two data points for $\sigma_{\rm reac}$ are best reproduced by the DGG-1 potential with $\chi^2/F \approx 2.9$ and an average deviation of only 3%. The worst description is obtained from the Nolte potential, with $\chi^2/F = 200$ and an average deviation of 22%. Most of the potentials under study reproduce the two experimental data points with average deviations between 5% and 10%, and average deviations above 15% are only found for the earlier Avrigeanu potential [31] and the Nolte potential [29], which has been optimized at much higher energies.

5. TALYS default

In addition, Fig. 2 includes the default TALYS combination of A-OMP: Watanabe [26] (Note that this will change to Avrigeanu [30] in the next versions.); N-OMP: Koning and Delaroche; GSF: Kopecky-Uhl generalized Lorentzian, M1 normalized; and LD: constant-temperature Fermi gas. The TALYS default calculation leads to an increased $\chi^2/F \approx 309$, which results from a significant overestimation of the $(\alpha,{\rm p})$ cross sections at low energies and a strong underestimation of the (α,γ) cross sections at all energies under study (see Fig. 2).

V. DISCUSSION

One main task in nuclear astrophysics is the determination of reaction rates $N_A\langle\sigma v\rangle$, which are essentially defined by the cross sections at low energies. In the present study we aim to use the above χ^2/F calculations to constrain the $^{64}{\rm Zn}(\alpha,\gamma)^{68}{\rm Ge}$ cross section for energies below the experimental data. Before this is done in the next Sec. V A, the results in the previous Sec. IV with $\chi^2/F \gg 1$ are discussed in more detail.

For the following discussion let us first assume that the statistical model is valid for $^{64}{\rm Zn}+\alpha$, and at least one hypothetical and *a priori* unknown combination of the almost 7000 combinations of input parameters is able to reproduce the experimental cross sections. Under these assumptions one should find that this hypothetical best-fit combination reproduces the experimental data with $\chi^2/F \lesssim 1$. For dominating statistical uncertainties of the experimental data, $\chi^2/F \approx 1.0$ should be found. For dominating systematic uncertainties, even cases with $\chi^2/F \ll 1$ may be found. Typical systematic uncertainties from charge integration, target thickness, or detector efficiency affect all data points in the same way (except the $\sigma_{\rm reac}$ from elastic scattering). Thus, for dominating systematic uncertainties, a variation of the absolute normalization of the experimental data within their common systematic uncertainty should lead to an almost-perfect agreement between the hypothetical best-fit combination and the normalized experimental data with $\chi^2/F \ll 1$.

In reality, the experimental data points are affected by both statistical and systematic uncertainties. For most of the data points, the systematic uncertainty is dominating; only for the weak (α,γ) channel and for low energies or energies slightly above the respective thresholds is the statistical uncertainty dominating [8]. Thus, we have varied the absolute normalization $N_{\rm exp}$ of the (α,γ), $(\alpha,{\rm n})$, and $(\alpha,{\rm p})$ cross sections within the range of $N_{\rm exp} = 0.7$–1.3, which corresponds to about three times the systematic uncertainty of the data, about 10% [8]. A smooth variation of the χ^2/F with the normalization factor $N_{\rm exp}$ was found, with a minimum of $\chi^2/F = 7.59$ for $N_{\rm exp} = 1.05$, compared to $\chi^2/F = 7.74$ for the original data ($N_{\rm exp} = 1.0$). Consequently, among the almost 7000 combinations of parameters for the StM calculations, there is no combination with $\chi^2/F \ll 1$, i.e., none of the almost 7000 combinations is able to reproduce the experimental data.

Strictly speaking, this means either that all almost 7000 combinations of input parameters are incompatible with the experimental results or that the chosen StM is inappropriate

in the present case. However, neither a better model for calculation of the ^{64}Zn $+\alpha$ reaction cross sections nor better parametrizations of the ingredients of the StM are available; this holds, in particular, for the A-OMPs under study which govern the theoretical uncertainties of the calculated low-energy cross sections. Nevertheless, low-energy cross sections have to be calculated, and their uncertainties have to be estimated, to provide an astrophysical reaction rate $N_A\langle\sigma v\rangle$ with a reasonable error bar. Therefore, the following considerations were used to obtain a realistic constraint for the low-energy (α,γ) cross section.

For dominating statistical uncertainties of the experimental data under study, the uncertainty of a fit parameter is calculated from the increase in χ^2 by 1. On the contrary, a dominating systematic uncertainty leads to a larger uncertainty for fit parameters because systematic uncertainties from many data points do not, on average, cancel each other. Thus, an increase of 1 in χ^2 for each data point should be used in the latter case; i.e., an increase of 1 in χ^2/F indicates the uncertainty of a fit parameter in the case of dominating systematic uncertainties. However, the above criteria both for χ^2 for statistical uncertainties and for χ^2/F for systematic uncertainties are robust only if $\chi^2/F \lesssim 1$ is achieved; but this was not possible in the present study of α-induced reaction cross sections of ^{64}Zn. Consequently, the available experimental data for ^{64}Zn cannot provide a strict mathematical constraint for the (α,γ) cross section at lower energies.

A reasonable criterion for the allowed range of χ^2/F has to be chosen to find a rather reliable constraint of the (α,γ) cross section at low energies. It should be pointed out here that this is not a new problem of the present study. The problem becomes very obvious here only because we attempt to provide a χ^2-based constraint of the (α,γ) cross section at low energies. In many previous papers the best combination of parameters was simply derived "by eye" from a comparison of experimental excitation functions with theoretical predictions using a more or less broad range of input parameters and/or computer codes for the StM. Then, often this best combination is simply used to calculate astrophysical reaction rates (without further discussion of χ^2).

Following the above discussion, we decided to use the following criterion for the allowed variation of χ^2. The best-fit combination of parameters reaches $\chi^2/F \approx 7.7$, corresponding to an average deviation of about 30% from the experimental data. For experimental uncertainties of the order of 10%, this means that we find an average deviation of almost 3σ. For the uncertainty determination of the low-energy (α,γ) data, we now accept all combinations of parameters with $\chi^2/F \leqslant 15$. This corresponds to an average $\approx 4\sigma$ deviation instead of the best-fit $\approx 3\sigma$ deviation; i.e., we allow for an increase in the average deviation of each data point by 1σ, and the resulting parameter space should describe the data with average deviations of less than about 40%.

A. Extrapolation to low energies

In the following we restrict ourselves here to estimation of the (α,γ) cross section at two energies below the lowest experimental point, at about 8 MeV. The first energy is chosen

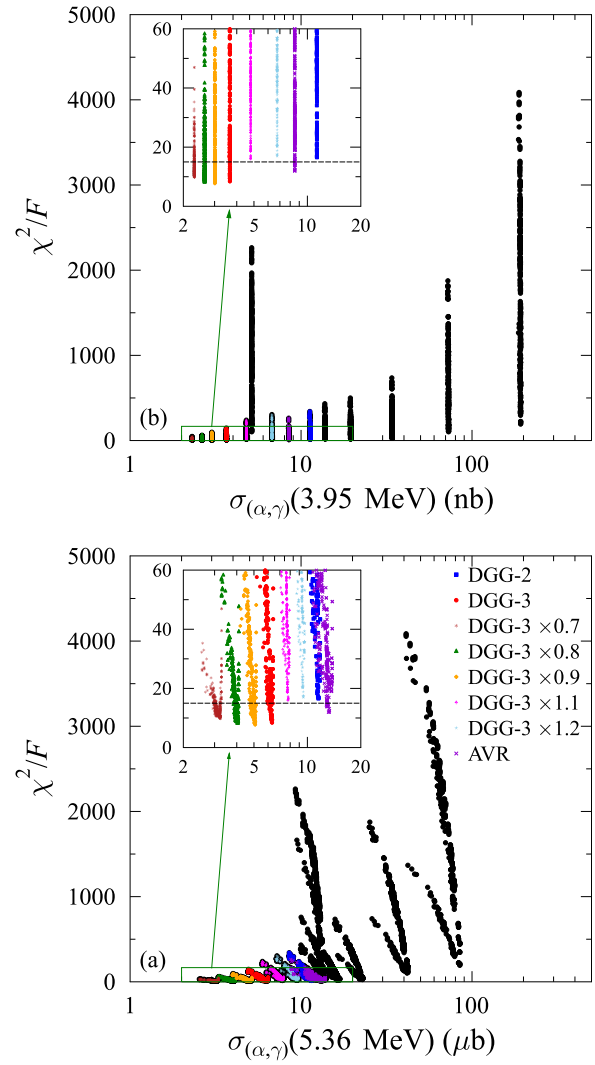

FIG. 3. χ^2/F as a function of the (α,γ) cross section (a) at 5.36 MeV (corresponding to the effective energy at $T_9 = 2.5$) and (b) at 3.95 MeV. Huge variations, between about 8 and 5000, are found for χ^2/F. Insets: All calculations with small $\chi^2/F < 60$. The chosen criterion $\chi^2/F \leqslant 15$ is indicated by the horizontal dashed line. For further discussion see the text.

from the most effective energy at $T_9 = 2.5$, i.e., a temperature of $T = 2.5 \times 10^9$ K, which is typical for the astrophysical p process. From the standard formulas, which are based on an energy-independent astrophysical S factor, the most effective energy at this temperature is $E_{\rm eff} \approx 5.36$ MeV. In practice, the assumption of a constant S factor is not realistic for heavy nuclei, and in most cases the effective energy is slightly shifted towards lower energies [44].

The second energy is taken as $E = 3.95$ MeV, which is slightly below the $(\alpha$,p) threshold and far below the $(\alpha$,n) threshold. At this low energy the (α,γ) cross section depends almost exclusively on the chosen A-OMP.

For the almost 7000 combinations of parameters, the calculated (α,γ) cross sections at 5.36 MeV vary between 2.5 and 85 μb. Figure 3(a) shows that the corresponding χ^2/F values vary between about 8 and almost 5000. The inset shows the

calculations with $\chi^2/F < 60$. Here it becomes clearly visible that the χ^2/F values are grouped according to the chosen A-OMP; e.g., the DGG-3 potential (with $N_{\rm DGG} = 1.0$, i.e., without further adjustment of the depth of the real part) favors (α,γ) cross sections between 4.9 and 6.5 μb (with the smallest χ^2/F for $\sigma \approx 6.3$ μb), and the AVR potential favors cross sections between 8.7 and 13.8 μb (with the smallest χ^2/F for $\sigma \approx 13.2$ μb). Adopting the above criterion of $\chi^2/F \leqslant 15$, we find 2.9 μb $\leqslant \sigma_{(\alpha,\gamma)} \leqslant 13.3$ μb at $E = 5.36$ MeV. Thus, the chosen criterion $\chi^2/F \leqslant 15$ restricts the (α,γ) cross section to $\sigma \approx 6$ μb with an uncertainty of a factor of 2, whereas the range of all calculations was between 2.5 and 85 μb.

The same procedure is repeated for the lower energy of 3.95 MeV [see Fig. 3(b)]. Here the predictions vary between 2.3 and 192 nb, i.e., the predictions cover almost two orders of magnitude. Applying the criterion $\chi^2/F \leqslant 15$ restricts the (α,γ) cross section to 2.3 nb $\leqslant \sigma_{(\alpha,\gamma)} \leqslant 8.5$ nb at $E = 3.95$ MeV, i.e., the (α,γ) cross section is $\sigma \approx 4.4$ nb, again with an uncertainty of about a factor of 2. Combinations of parameters which lead to much higher cross sections are excluded by the chosen χ^2 criterion.

As expected, the calculated cross section of the (α,γ) reaction depends almost exclusively on the A-OMP at the lower energy of 3.95 MeV. This is reflected by the strictly vertical grouping of the different A-OMPs in Fig. 3(b). At the slightly higher energy of 5.36 MeV, a grouping according to the A-OMPs is also observed. However, because the (α,γ) cross section is sensitive not only to the A-OMP, but also to other parameters, the grouping is not strictly vertical here [see Fig. 3(a)].

Finally, it is interesting to see that the few-parameter ATOMKI-V1 potential is only able to reach $\chi^2/F \approx 100$, but nevertheless, it is able to predict the low-energy (α,γ) cross sections reasonably well. At the higher energy of 5.36 MeV the ATOMKI-V1 potential predicts (α,γ) cross sections of between 9.3 and 13.5 μb, and at the lower energy of 3.95 MeV the (α,γ) cross section from ATOMKI-V1 is 5.1 nb.

VI. CONCLUSIONS

Excitation functions of the cross sections of the ^{64}Zn$(\alpha,\gamma)^{68}$Ge, ^{64}Zn$(\alpha,n)^{67}$Ge, and ^{64}Zn$(\alpha,p)^{67}$Ga reactions and the total reaction cross section $\sigma_{\rm reac}$ have been analyzed using the statistical model and a χ^2-based assessment of the underlying parameters. The best fit to the experimental data at low energies [7,8] shows $\chi^2/F \approx 7.7$ and an average deviation factor of about $f_{\rm dev} \approx 1.3$ from all experimental data.

The complete parameter space of the TALYS code was investigated using almost 7000 combinations of the α-nucleus OMPs, nucleon-nucleus OMPs, γ-ray strength functions, and level densities. The α-nucleus potential was identified as the most important ingredient of these StM calculations. This fact can be derived from the behavior of the χ^2/F. The best fit is obtained by a modification of the third version of the Demetriou *et al.* [28] potential where the real part is scaled by a factor of $N_{\rm DGG} = 0.9$. This best-fit result is still far from $\chi^2/F \approx 1$. A reduction of χ^2 should be achievable from further improvements of the α-nucleus OMP at low energies. $\chi^2/F \approx 1$ will probably not be reachable because of nonstatistical fluctuations of the reaction cross sections, in particular, for the ^{64}Zn$(\alpha,p)^{67}$Ga reaction at low energies.

From the range of χ^2/F values and the corresponding variation of the (α,γ) cross section at lower energies, an uncertainty of about a factor of 2 is estimated for the astrophysical reaction rate of the ^{64}Zn$(\alpha,\gamma)^{68}$Ge reaction and its cross section at very low energies. The uncertainty results from all reasonable fits with $\chi^2/F \leqslant 15$ and their extrapolations down towards astrophysically relevant energies where no experimental data for the ^{64}Zn$(\alpha,\gamma)^{68}$Ge reaction are available. Improved (α,γ) data at lower energies could reduce the uncertainty of the (α,γ) reaction rate and help to further constrain the parameters for statistical model calculations.

ACKNOWLEDGMENTS

This work is dedicated to Endre Somorjai on the occasion of his 80th birthday. We thank the members and collaborators of the Atomki Nuclear Astrophysics group—established by Endre Somorjai—for maintaining a fruitful and pleasant working atmosphere over many years. This work was supported by OTKA (Grant Nos. K108459 and K120666).

[1] P. Mohr, Zs. Fülöp, and H. Utsunomiya, Eur. Phys. J. **32**, 357 (2007).
[2] S. E. Woosley and W. M. Howard, Astrophys. J. Suppl. **36**, 285 (1978).
[3] M. Arnould and S. Goriely, Phys. Rep. **384**, 1 (2003).
[4] T. Rauscher, Phys. Rev. C **73**, 015804 (2006).
[5] W. Rapp *et al.*, Astrophys. J. **653**, 474 (2006).
[6] C. Travaglio, R. Gallino, T. Rauscher, N. Dauphas, F. K. Röpke, and W. Hillebrandt, Astrophys. J. **795**, 141 (2014).
[7] A. Ornelas, P. Mohr, Gy. Gyürky, Z. Elekes, Zs. Fülöp, Z. Halász, G. G. Kiss, E. Somorjai, T. Szücs, M. P. Takács, D. Galaviz, R. T. Güray, Z. Korkulu, N. Özkan, and C. Yalçın, Phys. Rev. C **94**, 055807 (2016).
[8] Gy. Gyürky, P. Mohr, Zs. Fülöp, Z. Halász, G. G. Kiss, T. Szücs, and E. Somorjai, Phys. Rev. C **86**, 041601(R) (2012).
[9] A. J. Koning, S. Hilaire, and S. Goriely, Computer code TALYS, version 1.8; http://www.talys.eu.
[10] P. Scholz, F. Heim, J. Mayer, C. Münker, L. Netterdon, F. Wombacher, and A. Zilges, Phys. Lett. B **761**, 247 (2016).
[11] E. Somorjai *et al.*, Astron. Astrophys. **333**, 1112 (1998).
[12] T. Rauscher, Int. J. Mod. Phys. E **20**, 1071 (2011).
[13] T. Rauscher and F.-K. Thielemann, At. Data Nucl. Data Tables **75**, 1 (2000).
[14] T. Rauscher, P. Mohr, I. Dillmann, and R. Plag, Astrophys. J. **738**, 143 (2011).
[15] P. Mohr, Phys. Rev. C **84**, 055803 (2011).
[16] T. Rauscher, Astrophys. J. Suppl. **201**, 26 (2012).
[17] T. Rauscher, Computer code NON-SMOKER; http://nucastro.org/websmoker.html.
[18] EXFOR database; http://www-nds.iaea.org/exfor.

[19] N. T. Porile, Phys. Rev. **115**, 939 (1959).
[20] F. H. Ruddy and B. D. Pate, Nucl. Phys. A **127**, 305 (1964).
[21] P. H. Stelson and F. K. McGowan, Phys. Rev. **133**, B911 (1964).
[22] M. Cogneau and L. J. Gilly, Nucl. Phys. **73**, 122 (1965).
[23] N. N. Abu Issa, A. E. Antropov, V. P. Gusev, P. P. Zarubin, A. A. Kolozhvari, and A. V. Smirnov, 39th Conference on Nuclear Spectroscopy and Nuclear Structure, Tashkent, USSR, 1989, p. 350 (unpublished).
[24] S. Mirzadeh and Y. Y. Chu, *Conference on Nuclear Data for Science and Technology, Jülich, Germany, 1991*, edited by S. M. Qaim (Springer Verlag, Berlin Heidelberg, 1992), p. 619.
[25] V. N. Levkovskij, *Activation Cross Section by Protons and Alphas* (Inter-Westi, Moscow, 1991).
[26] S. Watanabe, Nucl. Phys. **8**, 484 (1958).
[27] L. McFadden and G. R. Satchler, Nucl. Phys. **84**, 177 (1966).
[28] P. Demetriou, C. Grama, and S. Goriely, Nucl. Phys. A **707**, 253 (2002).
[29] M. Nolte, H. Machner, and J. Bojowald, Phys. Rev. C **36**, 1312 (1987).
[30] V. Avrigeanu, M. Avrigeanu, and C. Mănăilescu, Phys. Rev. C **90**, 044612 (2014).
[31] V. Avrigeanu, P. E. Hodgson, and M. Avrigeanu, Phys. Rev. C **49**, 2136 (1994).
[32] P. Mohr, G. G. Kiss, Zs. Fülöp, D. Galaviz, Gy. Gyürky, and E. Somorjai, At. Data Nucl. Data Tables **99**, 651 (2013).
[33] X.-W. Su and Y.-L. Han, Int. J. Mod. Phys. E **24**, 1550092 (2015).
[34] A. J. Koning and J. P. Delaroche, Nucl. Phys. A **713**, 231 (2003).
[35] J.-P. Jeukenne, A. Lejeune, and C. Mahaux, Phys. Rev. C **16**, 80 (1977).
[36] E. Bauge, J. P. Delaroche, and M. Girod, Phys. Rev. C **63**, 024607 (2001).
[37] S. Goriely and J.-P. Delaroche, Phys. Lett. B **653**, 178 (2007).
[38] D. M. Brink, Nucl. Phys. **4**, 215 (1957).
[39] P. Axel, Phys. Rev. **126**, 671 (1962).
[40] J. Kopecky and M. Uhl, Phys. Rev. C **41**, 1941 (1990).
[41] R. Capote *et al.*, Nucl. Data Sheets **110**, 3107 (2009).
[42] S. Goriely, Phys. Lett. B **436**, 10 (1998).
[43] A. J. Koning, S. Hilaire, and S. Goriely, Nucl. Phys. A **810**, 13 (2008).
[44] T. Rauscher, Phys. Rev. C **81**, 045807 (2010).